

Synthesis of polyaniline /CeO₂ nanocomposites as inhibitor coating on zinc: Evaluation of the corrosion behaviour

Messabhia Abdeslam* , Boudellioua Hichem² , Hamlaoui Youcef³

¹Chemical engineering Department, Physics of Matter and Radiation Laboratory, ¹ Mohamed Chérif Messaadia de Souk Ahras University, Souk Ahras 41000 Algeria.

²Chemical engineering Department, Physics of Matter and Radiation Laboratory, ¹ Mohamed Chérif Messaadia de Souk Ahras University, Souk Ahras 41000 Algeria.

³Chemical engineering Department, Physics of Matter and Radiation Laboratory, ¹ Mohamed Chérif Messaadia de Souk Ahras University, Souk Ahras 41000 Algeria.

a.messabhia@univ-soukahras.dz

Abstract – In this study, Polyaniline/ceria nanoparticles (PANI/CeO₂) nanocomposite (NPs) were prepared by in situ polymerization of aniline in the presence of CeO₂ NPs . Ceria nanoparticles were produced via the precipitation of cerium Ce(NO₃)₃.6H₂O in water where the average hydrodynamic diameter of the obtained nanoparticles was about 8 nm (determined by nanosizer) . Infrared spectroscopy “FTIR” and white light interferometry analysis were used to characterize the obtained PANI/CeO₂ and also the electrodeposited coatings. To overcome the low solubility of the polymer /ceria nanoparticles, the composites was dissolved in dimethyl sulfoxide solvent under ultrasonic stirring. The electrochemical behavior of zinc substrate in the corrosive medium with and without PANI / CeO₂ addition was studied using d.c polarization techniques and electrochemical impedance spectroscopy “EIS”. All the obtained results have shown the good behavior of PANI/CeO₂ in the protection of zinc against corrosion. Indeed, the addition of 66 ppm of PANI / CeO₂ to the aggressive solution 0.5N NaCl provides to the substrate an electrochemical efficiency about of 77.74%. It has been shown that PANI /CeO₂ acts on the anodic process. the hybrid PANI/ CeO₂ NPs can be considered as an interesting way to enhance the protection performance of the PANI/CeO₂ on zinc.

Keywords –D.C Polarization, Nanosizer, EIS, Composite

I. INTRODUCTION

Since the first investigations reported by Deberry [1] in 1984, showing that Polyaniline (PANI) can be considered a promising anticorrosion material, conductive polymers, such as PANI [2] polypyrrole (PPy) [3] have been used to provide corrosion protection for many metals. However, PANI has attracted much attention due to its ease of synthesis, good stability, and redox-free acid/base doping process [4]. In all previous work, it was concluded that conducting polymers act both by forming a physical barrier between the surface of the substrate and the aggressive media and by anodic protection

[5]. Wessling et al [6] proposed that PANI and PPy coatings may possess a self-healing nature for the passive oxide between the substrate metal and the coating, which could be spontaneously reformed at the defective locations by the oxidative ability of the conductive polymer. more studies have been carried out to improve the corrosion resistance of PANI coatings by incorporating nanoparticles, such as TiO₂ [7], and ZnO [8]. Among these nano-oxides, CeO₂ is considered as an effective corrosion inhibitor and has attracted considerable interest to replace toxic chromates [9]. For example, Montemor [10] added CeO₂ and Ce³⁺ to the silane

film on galvanized steel and showed that film stability is improved in presence of CeO₂.

In this work, PANI/CeO₂ NPs were synthesized. The corrosion performance of PANI/CeO₂ coatings formed onto the surface of the zinc electrode was evaluated in sodium chloride electrolyte.

I. MATERIALS AND METHOD

Aniline (100%) GPR RECTAPUR, ammonium persulfate (99.7%) GPR RECTAPUR, acetic acid, hydrochloric acid (37%) AnalaR NORMAPUR, dimethyl (Min 99%) Biochim Chemopharma, methanol (99,90%) Honeywell, Sodium chloride (99,90%) Sigma – Aldrich Canda, ethanol AnalaR NORMAPUR.

A number of methods are used both to study the corrosion of zinc in a saline medium (NaCl) and to verify the efficiency of the composite (polyaniline - CeO₂) against corrosion. We are interested in chemical and electrochemical methods and principally in using FTIR and white light interferometry analysis were used to characterize the obtained PANI/CeO₂, d.c polarization techniques and electrochemical impedance spectroscopy “EIS”

A. Preparation of Soluble polyaniline Salt

A 200 ml binary solvent mixture was prepared by mixing 80 ml of acetic acid with 17 ml of concentrated HCl (37%o) and 113 ml of H₂O in a flask. Thereafter, 3.84 g of aniline was mixed with 140 ml of the prepared binary solvent and stirred constantly in an ice bath. Ammonium peroxydisulfate solution (9.12 g of APS dissolved in 60 ml of the binary solvent) was added dropwise into the aniline solution. The reaction mixture was stirred continuously in an ice bath for 2 h, then filtered and washed with deionized water and methanol, and dried under vacuum at 70 °C for 12 h [11].

In order to make the obtained polymer soluble in the aqueous medium and also to improve its anticorrosive performance some solutions mainly the modification of the synthèse way have been considered. Among the modification techniques, doping, copolymerization, layering, and combination with substances that can exert a synergistic effect and compositing [12].

B. Synthesis of CeO₂ NPs

All chemical reagents were used without further purification. Synthesis of cerium oxide nanoparticle were prepared using cerium nitrate (Ce(NO₃)₃.6H₂O, Strem, 99.9%) as precursor in the presence of acetic acid. In the synthesis process, 0.5M cerium nitrate and 0.5M acetic acid were dissolved in 100 ml distilled water in a double-walled reactor under magnetic stirring for 10 min. After raising the temperature of the solution to 60°C, an aqueous solution of ammonia (NH₄OH) at 24.5% was added dropwise while keeping the reactor under stirring until reaching a pH equal to 9 where the temperature of the reactor was further increased to 90°C and immediately afterwards it was closed in order to reduce the percentage of oxygen almost to 50%. After 24 hours of stirring as reaction time, the precipitate which is the particles of cerium oxides is recovered by centrifugation at 4000 rpm for 50 minutes and in the presence of excess ethanol. Then, in order to eliminate the residual ions, the precipitate obtained is washed and centrifuged with distilled water and ethanol alternately three times, finally, the precipitate is dried at 60°C for 24h, and finally, the solid obtained was ground to fine size particles with a hydrodynamic diameter of about 8 nm were obtained using a nanosizer (Fig. 1)

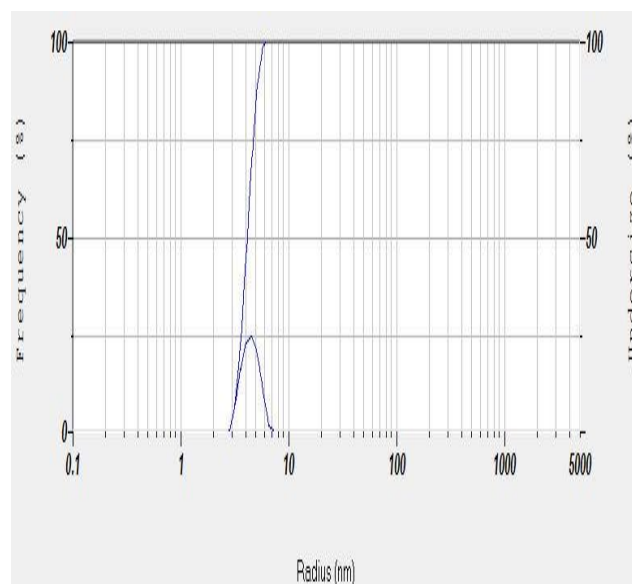


Fig. 1 Size distribution of CeO₂ particles by nanosizer

C. In situ polymerization of doped PANI NPs

To prepare the CeO₂-PANI composite was synthesized by in situ polymerization, 0.5 g of CeO₂ was ultrasonically dispersed in 200 ml of 1.0 M HCl for 1 h under ambient conditions to obtain a dark

suspension. The suspension was then cooled to 2 °C in an ice water bath, and 5 ml of aniline monomer was injected into the suspension and dispersed for 1 h under strong stirring. Then, an equal volume of 0.25 M ammonium persulfate solution (APS) was added dropwise to the above mixture and kept at 0 °C - 4 °C for 24 h. Finally, the PANI/CeO₂ NPs were washed with distilled water and ethanol and dried in a vacuum oven at 60 °C for 24 h [13].

I. RESULTS

Infrared spectroscopy spectra highlighted that the obtained composite is emeraldine salt reinforced by cerium oxide.

it is observed that the addition of low amount of inhibitor shifts the E_{corr} to anodic values (-1.0071V/ECS). which confirms the anodic behaviour of this composite.

EIS has shown that the efficiency of the addition of PANI / cerium oxide in the aggressive solution can exceed 82,44%. at a concentration of 66 ppm.

The surface morphology examined by MO and WLI has shown that the increase in the inhibitor concentration allowed to an increase the average thickness of the film which is in good agreement with the electrochemical results showing the good behaviour of PAN/CeO₂ I as inhibitor of zinc corrosion.

II. DISCUSSION

A. FTIR analysis

The FTIR spectra of PANI and composite PANI-CeO₂ are shown in (Fig.2) in the PANI spectrum, first, we note that the weak band appearing at 3249.43 cm⁻¹ is attributed to the symmetric elongation of the (NH) group. The two intense bands at 1497.49cm⁻¹ - 1585.04cm⁻¹, are respectively associated with the nitrogen-benzenoid-nitrogen system (N-B-N) and nitrogen-quinoid-nitrogen system (N=Q=N) vibrations of the polymer. These bands are very important since they provide qualitative information on the degree of oxidation of polyaniline

the band at 1310.53cm⁻¹ is due to vibrations of the C-N bond in particular groupings of the benzenoid and quinoid systems. In addition, we note that the absorption band at 1149.76 cm⁻¹ is associated with the (-NH+=) vibration. This band indicates the high degree of electron delocalization on the polyaniline structure and thus confirms the protonation of emeraldine.

Finally, the band located at 834.74 cm⁻¹ is attributed to the deformation of the C-H out of the plane for the benzene rings substituted in position 1 and 4, in the composite PANI -CeO₂ spectrum, The bands obtained were in good agreement with literature we observe an intense absorption band at 3742.81 cm⁻¹ characteristic of free OH bond, the band 1743.73 cm⁻¹ characteristic of CO bond of carboxylic acid. The band at 2356.58 cm⁻¹ due to the absorption of atmospheric CO₂. The band in the range of 473, 32 cm⁻¹ are related to Ce-O vibrations.

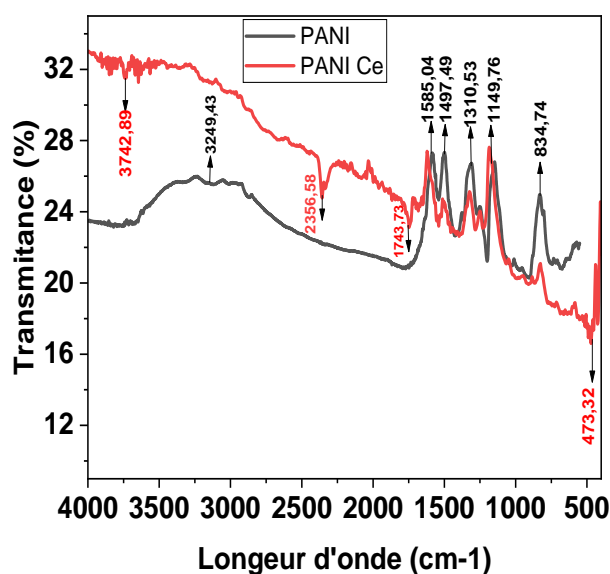


Fig. 2 IR spectra of PANI and PANI /CeO₂ composite

B. Open circuit potential measurement

(Fig.3) shows the zinc abandonment potential during 17 h of immersion. The evolution of the potential for the test performed without composite inhibitor characterizes the corrosion of the sample with formation of the corrosion products on the surface of the substrate. At different concentrations of doped polyaniline, we observe that the corrosion potential (E_{corr}) tends to stabilize after 11 h of immersion in the different concentrations of CeO₂ doped polyaniline, thus the increase in concentration of doped PANI/CeO₂ in the 0.5M NaCl solution shifts (E_{corr}) from -1.033V/ECS to more electronegative values around -1.083 V/ECS, value reached after immersion of the substrate in 33 ppm PANI/CeO₂. This is certainly related due to the formation of a PANI-based coating on the electrode surface. However, by increasing the concentration

of cerium oxide enhanced inhibitor to around 66 ppm, the corrosion potential (E_{corr}) increased until it stabilized at -1.054 V/ECS.

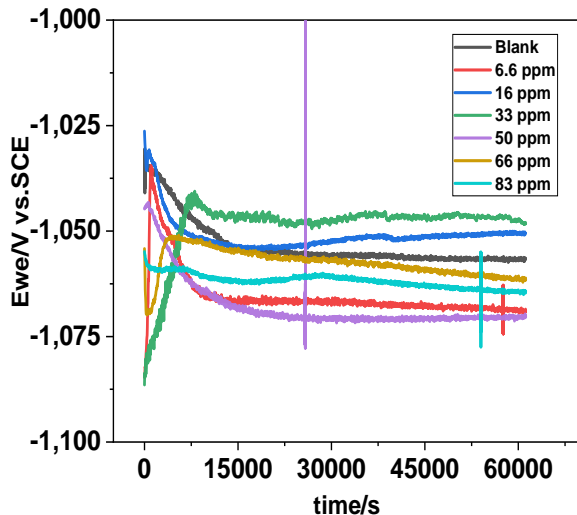


Fig. 3 Evolution of the abandonment potential as a function of immersion time in 0.5 N NaCl without and with cerium oxide-doped polyaniline addition.

C. Polarization curve

(Fig.4) shows the polarization curves established in 0.5N NaCl in the presence of different concentrations of composite (CeO₂-doped PANI). The plots of the polarization curves were made from the most commonly used techniques in electrochemistry to determine the polarization resistance and the corrosion rate. Indeed, the Tafel plots allow us to directly access the values of the current densities.

Table I: recapitulates the different electrochemical parameters deduced from the polarization curves as well as the inhibitory efficiency E (%) calculated from the following relation:

$$E (\%) = \frac{I_{Corr} - I_{Corr(inh)}}{I_{Corr}} \times 100 \quad (1)$$

Where I_{corr} and $I_{corr}(inh)$: are respectively the values of the corrosion current densities without and with addition of the inhibitor.

The addition of increasing amounts of PANI/CeO₂ composite in solution in 0.5N NaCl seems to induce a continuous decrease in the corrosion current density. Moreover, it is observed that the addition of low amount of inhibitor shifts the E_{corr} to anodic

values (-1.0071V/ECS). which confirms the anodic behavior of this composite. have proposed that the electrochemistry of conductive polymers is responsible for the anodic protection of the substrate metals and the stabilization of the polymer coatings against cathodic delamination. Anodic protection occurs by shifting the corrosion potential to the passive region for the relevant metal in the relevant electrolyte [1]. despite the cerium oxide and cathodic behavior. By calculating the corrosion current densities without and with the addition of inhibitor. we found that the protective power increases as the inhibitor concentration increases. The maximum protection is reached 77.45% at a concentration of 66 ppm. As we observe that the polyaniline composite oxidizes cerium. forming a protective layer minimizing the rate of zinc dissolution. The reduction of oxygen to hydroxide that moves from the metal surface to the polymer/electrolyte interface and probably due to the re-oxidation of the conductive polymer.

CeO₂ nanoparticles also produce a self-healing effect on smart coatings. moreover CeO₂/polymer. Several research papers have highlighted the improved corrosion inhibition performance of the hybrid [12].

Table. 1 Electrochemical parameter deduced from the polarization curves

| Inhibitor concentration ion mg/L | E_{corr} (mV/ECS) | Ba (mV) | Bc (mV) | Rp (Ω) | I ($\mu A/Cm^2$) | E % |
|----------------------------------|---------------------|---------|----------|-----------------|--------------------|-------|
| Blank | -1035.34 | 17.7 | 149 | 209 | 41.92 | |
| 6.6 | -1034.79 | 23.5 | 359.9 | 356 | 34.54 | 17.60 |
| 16 | -1028.074 | 28.7 | ∞ | 466 | 34.33 | 18.10 |
| 33 | -1040.38 | 17.4 | 105.3 | 345 | 23.97 | 42.82 |
| 50 | -1029.82 | 18.7 | 115.9 | 604 | 14.76 | 64.79 |
| 66 | -1008.91 | 14.9 | ∞ | 883 | 9.34 | 77.45 |
| 83 | -1012.36 | 16.5 | ∞ | 372 | 24.56 | 41.41 |

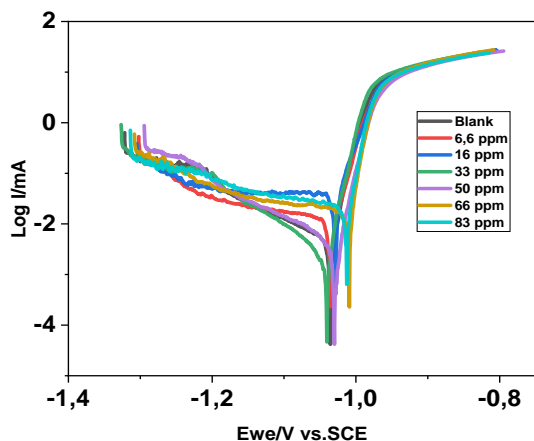


Fig.4 Zinc polarization curves at different inhibitor concentrations in 0.5N NaCl

D. Electrochemical impedance spectroscopy

Additional information of the corrosion behaviour, EIS diagrams have been performed in the same conditions mentioned above. Indeed, EIS translates the electrochemical contribution of the system to the observed electrical response. It allows a more complete analysis of the mechanism of the inhibitor action compared to the d.c polarization methods. It also allows separating the different mechanisms involved in the inhibition process where the properties of the film as well as the mechanism of charge transfer can be identified and quantified. Depending on the different parameters imposed on the system.

The impedance diagrams of the Zn coatings at their corrosion potential have also been obtained in NaCl solution without and with inhibitor addition (Fig. 5). The physical values were fitted with the Zview software through appropriate equivalent circuits (see Fig. 5a) and the results are gathered in Table. It is clear that for the shortest immersion times the obtained diagrams display three relaxation times, two capacitive loops at high middle frequencies and the beginning of a LF inductive loop. In agreement with the Nyquist diagrams, the Bode plots obtained with and without inhibitor addition (Fig. 5b) show two time-constants well defined at around 100 and 0.1 Hz before immersion and a third one not well defined at low frequencies.

At first view, the polarization resistances “Rp” values calculated at low frequency at the

intersection with Zre axis and (Table. 2) and the charge transfer resistance “Rct” leads us to conclude that the addition of the inhibitor brings to an improve in the corrosion efficiency where a maximum is observed after addition of 66 mg/l. However, the film resistance values shows that the maximum value is observed at 33ppm. This is may indicate that in the presence of 33 ppm the deposited film is compact becoming porous at higher concentrations. It is noted that the CPEc and CPEDl (constant phase element) are the non-ideal (dispersive) layer capacitance and double layer capacitance, respectively; Rct is the charge transfer resistance, and Rs corresponds to the resistance of the electrolyte. The loop at HF (higher frequencies) is typically related to the layer resistance, and the one at MF (lower frequencies) to the corrosion process itself. However, the relaxation time observed at LF is attributed to the relaxation phenomena occurring at the electrode surface. The main surface reactions are due to the formation and growth of the passivation film modifying the surface coverage rate. This phenomenon is generally modelled by either an induction band or a capacitor in parallel with a negative resistance.

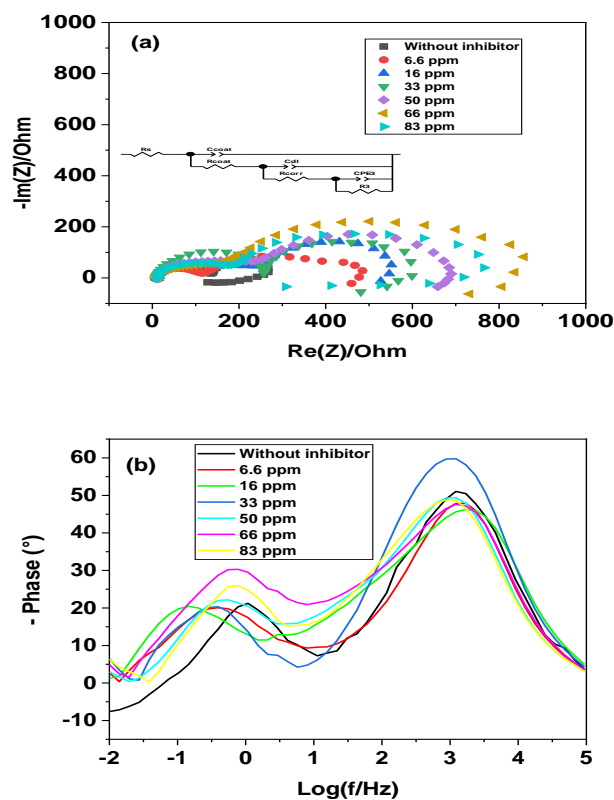


Fig. 5 EIS plots (a) Nyquist and (b) phase plots performed on Zn Substrate at different PANI/CeO₂ concentrations and at room temperature.

Table. 2 EIS parameters obtained on Zn substrate immersed in NaCl 0.5 N with and without inhibitor addition at room temperature.

| Cc (ppm) | Rs Ω.c m ² | CPEc μFs ⁽ⁿ⁾ cm ⁻² | nc | Rc Ωcm ² | CPE dl mFs ⁽ⁿ⁾ cm ⁻² | ndl | Rct Ω.cm ² | C F cm ⁻² | R3 Ω.c m ² | Rp Ω.cm ² | E % |
|----------|-----------------------|--|------|---------------------|--|------|-----------------------|----------------------|-----------------------|----------------------|-------|
| Blank | 9.01 | 15.27 | 0.85 | 127.1 | 1.72 | 0.96 | 138.9 | -0.0260 | -119 | 129.0 | / |
| 6.6 | 8.81 | 18.92 | 0.84 | 104.6 | 3.91 | 0.72 | 297.7 | -0.0180 | -78 | 460.1 | 53.34 |
| 16 | 6.68 | 93.53 | 0.64 | 233.4 | 4.49 | 1.00 | 293.1 | -0.0490 | -20 | 527.3 | 52.61 |
| 33 | 8.36 | 11.03 | 0.88 | 254.9 | 2.54 | 1.00 | 315.0 | -0.0235 | -117 | 484.1 | 55.90 |
| 50 | 10.1 | 45.55 | 0.74 | 214.2 | 1.34 | 0.84 | 463.2 | -0.0234 | -128 | 659.4 | 70.01 |
| 66 | 6.83 | 50.06 | 0.74 | 139.7 | 1.20 | 0.66 | 791.2 | -0.0190 | -211 | 734.7 | 82.44 |
| 83 | 8.71 | 42.96 | 0.77 | 179.1 | 1.12 | 0.84 | 521.1 | -0.013 | -460 | 309.6 | 73.34 |

E Surface morphology

The protection afforded by the inhibitor addition was evaluated by analysing the morphology of the surface of the substrate after polarisation test in the aggressive medium by optical microscope “MO” and white light interferometer “WLI”. The MO images (Fig. 6) and WLI measurements where the results are presented in the three-dimensional (3D) images shown in (Fig.7) show that the samples without an inhibitor undergo a partial dissolution (black areas). This agrees with previous works showing that Zn substrate describe a poor corrosion resistance in saline medium. However, in the presence of the corrosion inhibitor, the MO images presented in Figure 6 show the deposition of a thin protective layer but not covering the entire surface of the substrate, which is in good agreement with WLI images. The calculated parameters of the film are gathered in Table 3. It is clear from the WLI images that the average thickness of the deposited film increases with increasing the inhibitor concentrations where the highest film thickness is observed when 66 ppm is added. Inversely it seems that the increase of the inhibitor concentration decreases the grain size and the roughness of the surface of the obtained deposits, which may be due to the formation of a deposit rich in inhibitor and free from corrosion product.

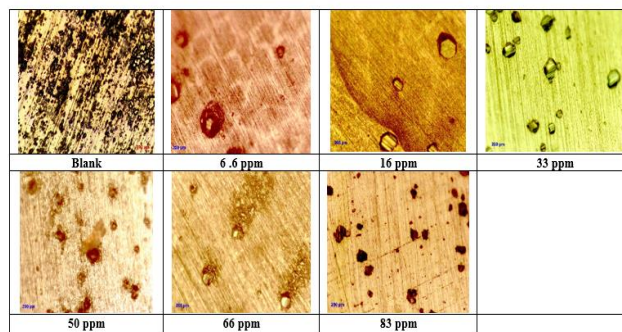


Fig. 6 optical microscope observations of the surface of zinc electrode after polarization in 0.5N NaCl solution in the absence and presence of different concentrations of ceria-doped polyaniline

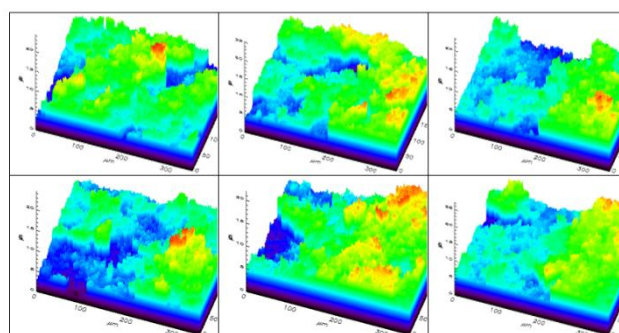


Fig. 7 WLI images (3 D) of the surface of zinc electrode after polarization in 0.5N NaCl solution in the absence and presence of different concentrations of ceria-doped polyaniline.

Table 3 Surface parameters of the substrate after polarization tests realized in 0.5M NaCl with the presence of different inhibitor concentration at room temperatures.

| Cc (ppm) | Average Thickness (μm) | Grain size (μm) | Roughness (μm) |
|----------|------------------------|-----------------|----------------|
| 6.6 | 4.49 | 0.0348 | 0.621 |
| 16 | 5.167 | 0.0269 | 0.594 |
| 33 | 5.196 | 0.0135 | 0.403 |
| 50 | 5.512 | 0.0129 | 0.548 |
| 66 | 5.721 | 0.0102 | 0.498 |
| 83 | 5.683 | 0.0144 | 0.435 |

III. CONCLUSION

In this work, soluble PANI/nanoceria in dimethyl sulfoxide was synthesized through chemical way where cerium oxide nanoparticles synthesized by precipitation method with a particle diameter about of 8 nm. Infrared spectroscopy spectra highlighted that the obtained composite is emeraldine salt

reinforced by cerium oxide. The inhibitory efficiency was verified by d.c polarisation and electrochemical impedance spectroscopy in saline medium 0.5N NaCl. The polarization curves show that the inhibitor shifts the substrate corrosion potential to anodic values suggesting the polyaniline/cerium oxide in dispersion acts by an adsorption mechanism on the zinc surface leading to an anodic protection. EIS has shown that the efficiency of the addition of PANI / cerium oxide in the aggressive solution can exceed 77,45%. The surface morphology examined by MO and WLI has shown that the increase in the inhibitor concentration allowed to an increase the average thickness of the film. Contrarily, the average roughness and the grain size raised. The film seemed to be more heterogeneous and containing cracks with increasing inhibitor concentration.

References

- [1] D. W. DeBerry. "Modification of the Electrochemical and Corrosion Behavior of Stainless Steels with an Electroactive Coating." *J. Electrochem. Soc.*, vol. 132, no. 5, pp. 1022–1026, 1985. doi: 10.1149/1.2114008.
- [2] T. Schauer, A. Joos, L. Dulog, and C. D. Eisenbach. "Protection of iron against corrosion with polyaniline primers." *Prog. Org. Coatings*, vol. 33, no. 1, pp. 20–27, 1998. doi: 10.1016/S0300-9440(97)00123-9.
- [3] Y. H. Lei, N. Sheng, A. Hyono, M. Ueda, and T. Ohtsuka. "Electrochemical synthesis of polypyrrole films on copper from phytic solution for corrosion protection." *Corros. Sci.*, vol. 76, pp. 302–309, 2013. doi: 10.1016/j.corsci.2013.07.003.
- [4] J. S. M. da Silva, S. M. de Souza, G. Trovati, and E. A. Sanches. "Chloride salt of conducting polyaniline synthesized in the presence of CeO₂: Structural analysis of the core-shell nanocomposite." *J. Mol. Struct.*, vol. 1127, pp. 337–344, 2017. doi: 10.1016/j.molstruc.2016.07.114.
- [5] G. M. Spinks, A. J. Dominis, G. G. Wallace, and D. E. Tallman. "Electroactive conducting polymers for corrosion control: Part 2. Ferrous metals." *J. Solid State Electrochem.*, vol. 6, no. 2, pp. 85–100, 2002. doi: 10.1007/s100080100211.
- [6] Wessling B. "Passivation of Metals by Coating with Polyaniline: Corrosion Potential Shift and Morphological Changes." *Adv. Mater.*, vol. 6, no. 3, pp. 226–228, 1994.
- [7] J. F. Pagotto, F. J. Recio, A. J. Motheo, and P. Herrasti. "Multilayers of PANi/n-TiO₂ and PANi on carbon steel and welded carbon steel for corrosion protection." *Surf. Coatings Technol.*, vol. 289, no. 2016, pp. 23–28, 2016. doi: 10.1016/j.surfcoat.2016.01.046.
- [8] M. Ibrahim et al.. "Enhanced corrosion protection of Epoxy/ZnO-NiO nanocomposite coatings on steel." *Coatings*, vol. 10, no. 8, 2020. doi: 10.3390/COATINGS10080783.
- [9] N. Pirhady Tavandashti, M. Ghorbani, A. Shojaei, Y. Gonzalez-Garcia, H. Terryn, and J. M. C. Mol. "PH responsive Ce(III) loaded polyaniline nanofibers for self-healing corrosion protection of AA2024-T3." *Prog. Org. Coatings*, vol. 99, pp. 197–209, 2016. doi: 10.1016/j.porgcoat.2016.04.046.
- [10] M. F. Montemor and M. G. S. Ferreira. "Cerium salt activated nanoparticles as fillers for silane films: Evaluation of the corrosion inhibition performance on galvanised steel substrates." *Electrochim. Acta*, vol. 52, no. 24, pp. 6976–6987, 2007. doi: 10.1016/j.electacta.2007.05.022.
- [11] K. Tzou and R. V. Gregory. "A method to prepare soluble polyaniline salt solutions - insitu doping of PANI base with organic dopants in polar solvents." *Synth. Met.*, vol. 53, no. 3, pp. 365–377, 1993. doi: 10.1016/0379-6779(93)91106-C.
- [12] S. A. Umoren and M. M. Solomon. "Protective polymeric films for industrial substrates: A critical review on past and recent applications with conducting polymers and polymer composites/nanocomposites." *Prog. Mater. Sci.*, vol. 104, no. March, pp.
- [13] Y. Lei et al.. "Polyaniline/CeO₂ nanocomposites as corrosion inhibitors for improving the corrosive performance of epoxy coating on carbon steel in 3.5% NaCl solution." *Prog. Org. Coatings*, vol. 139, no. October, p. 105430, 2020. doi: 10.1016/j.porgcoat.2019.105430.